UNIVERSITY OF LEEDS

This is a repository copy of *Misconceptions and generalizations of the Den Hartog galloping criterion*.

White Rose Research Online URL for this paper:
http://eprints.whiterose.ac.uk/80834/

Version: Accepted Version

Article:
Nikitas, N and Macdonald, JHG (2014) Misconceptions and generalizations of the Den Hartog galloping criterion. Journal of Engineering Mechanics, 140 (4). 04013005. ISSN 0733-9399

https://doi.org/10.1061/(ASCE)EM.1943-7889.0000697

Reuse
Unless indicated otherwise, fulltext items are protected by copyright with all rights reserved. The copyright exception in section 29 of the Copyright, Designs and Patents Act 1988 allows the making of a single copy solely for the purpose of non-commercial research or private study within the limits of fair dealing. The publisher or other rights-holder may allow further reproduction and re-use of this version - refer to the White Rose Research Online record for this item. Where records identify the publisher as the copyright holder, users can verify any specific terms of use on the publisher's website.

Takedown
If you consider content in White Rose Research Online to be in breach of UK law, please notify us by emailing eprints@whiterose.ac.uk including the URL of the record and the reason for the withdrawal request.

White Rose university consortium
Universities of Leeds, Sheffield & York

eprints@whiterose.ac.uk
https://eprints.whiterose.ac.uk/

Misconceptions and generalisations of the Den Hartog galloping criterion

N. Nikitas[a,*], J.H.G. Macdonald[b,]

[a] *Lecturer, University of Bristol, Department of Civil Engineering, Queen's Building, University Walk, Bristol, BS8 1TR, UK*
[b] *Reader, University of Bristol, Department of Civil Engineering, Queen's Building, University Walk, Bristol, BS8 1TR, UK*

Abstract

Classical quasi-steady galloping analysis deals exclusively with cases of across-wind vibrations, leaving aside the more general situation where the wind and motion may not be normal. This can arise in many circumstances, such as the motion of a power transmission cable about its equilibrium configuration, which is swayed from the vertical plane due to the mean wind, or for a tall slender structure in a skewed wind. Furthermore the generalisation to such situations, when this had been made, has only considered special issues. In this paper the correct equations for the quasi-steady aerodynamic damping coefficients for the rotated system or wind are derived, and differences from other variants are highlighted. Motion in two orthogonal structural planes is considered, potentially giving coupled translational galloping, for which previous analysis has often been limited or has even arrived at erroneous conclusions. For the two-degree-of-freedom case, the behaviour is dependent on the structural as well as aerodynamic parameters, in particular the orientation of the principal structural axes and the relative natural frequencies in the two planes. For the first time, differences in the aerodynamic damping and zones of galloping instability are quantified, between solutions from the correct perfectly tuned, well detuned and classical Den Hartog equations (and also an incorrect generalisation of it), for a variety of typical cross-sectional shapes. It is found that although the Den Hartog summation often gives a reasonable estimate for the actual aerodynamic damping even for the rotated situation, in some circumstances the differences can be quite large.

Keywords: Galloping, Den Hartog, quasi-steady theory, aerodynamic damping, translational coupling

1. Introduction

Quasi-steady theory allows aerodynamic problems to be simplified vastly by replacing the actual unsteady condition in hand by an equivalent static one, where only the relative flow velocity is considered for capturing

*Corresponding author. Tel.: +44 113 343 0901; fax: +44 113 343 2265
Email addresses: N.Nikitas@leeds.ac.uk (N. Nikitas), John.Macdonald@bristol.ac.uk (J.H.G. Macdonald)

the relevant aerodynamic forcing. Its most famous application is probably the galloping criterion put forward by Den Hartog (1932, 1947) setting the condition for aerodynamically unstable behaviour of a single degree-of-freedom (DOF) oscillator as:

$$F' = \sin\alpha\,(-L + D') + \cos\alpha\,(L' + D) < 0 \tag{1}$$

which is often (e.g. see Holmes (2001, p117), Hémon and Santi (2002, p856)) expressed in terms of static force coefficients as:

$$S_{\rm sc} = \sin\alpha\,(-C_L + C'_D) + \cos\alpha\,(C'_L + C_D) < 0 \tag{2}$$

where α is the angle of attack, L, D, C_L, C_D are the static lift and drag forces and static lift and drag coefficients respectively, assumed for nominally 2D flow to be functions only of α, and the prime indicates the derivative with respect to α. The criterion is only a condition to avoid an undamped oscillator becoming negatively damped due to aerodynamic action. Thus the overall dynamic stability problem simply involves determining the aerodynamic damping contribution and setting it equal and opposite to the available structural damping. However, Eq.(2) when presented as such is misleading as it has a major limitation. It is only valid for $\alpha = 0$, corresponding to 1D oscillations normal to the wind direction, which is tacitly ignored. In the general case (i.e. $\alpha \neq 0$), the principal structural axes may not be aligned along the flow direction and normal to it, for example for a vertical section in skewed wind (or for a horizontal section in inclined wind) in bending as in Fig.1(a), or considering the static sway of a catenary due to the mean wind force, Fig.1(b). Then Eq.(2) fails to correctly account for the effect of aerodynamic damping, as in the across-wind galloping scenario, and even if employed in its correct Den Hartog stated form then it fails to describe the true condition. The correct treatment for 1 degree-of-freedom (DOF) galloping not necessarily normal to the wind, although sketched in the literature previously (Richardson and Martuccelli (1965), Blevins (1977)), is generally not followed in practice and the resulting errors in calculations arising from the mishandling have not previously been quantified. To this end a number of benchmark cross-sections are considered to illustrate the differences emerging in defining instability bounds.

In addition, the full extension of generalised translational galloping analysis to sections with principal axes arbitrarily inclined to the flow, has to cover motion in both axes, including their aerodynamic coupling, which is especially important when they have close natural frequencies. Such an analysis has previously been performed by a number of authors with specific omissions and sometimes with erroneous conclusions. In particular, Jones (1992) addressed coupled motion in two planes in some detail, but only for the special case

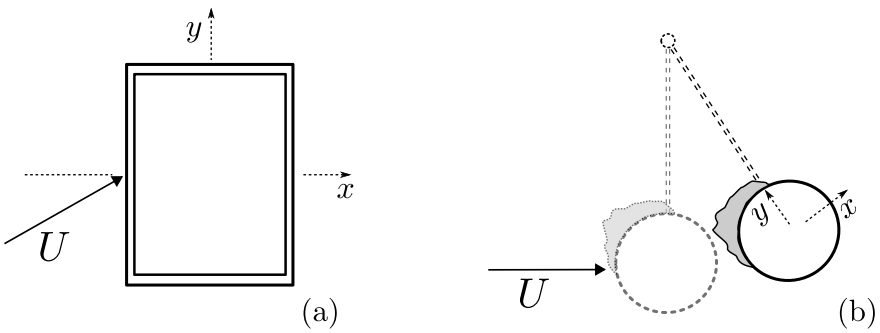

Figure 1: (a) Plan view; vertical section in skewed wind (or elevation; horizontal section in inclined wind) in bending (b) Catenary swaying statically due to the mean wind force. Note x and y are the principal structural axes, which sometimes coincide with axes of symmetry, as in (a), but not necessarily so.

of $\alpha = 0$ with identical natural frequencies in the vertical and horizontal directions, and she concluded that no vertical galloping can occur when horizontal motion is restrained. Although suggesting that this may be a reason for experimental behaviour observed, it results only from mistreating the boundary conditions and neglecting the effect of the envisaged horizontal restraining force in the analysis. Liang et al. (1993) and Li et al. (1998) used the formulation in terms of body co-ordinates, following Davenport (1966), and covered the seemingly more general case of $\alpha \neq 0$ 2D perfectly tuned coupled motion. However, the fact that the frequencies are restrained to be tuned renders α arbitrary, thus the results are only equivalent to Jones' (1992) case and not a generalisation of it. By using force coefficients defined in body co-ordinates rather than wind co-ordinates, the connections of their work to the Den Hartog criterion are unclear. In the analysis a special behavioural subcase is missed and the incorrect assertion is put forward that 2D coupled galloping oscillations may occur only when the fundamental natural frequencies of a structure in the two orthogonal principal directions are identical, which is a consequence of erroneously assuming that the motion in the two planes should be in phase. Macdonald and Larose (2008a,b), focusing on dry inclined galloping of circular cables, accurately provided the full 2D aerodynamic damping matrix, including also terms due to force coefficient variations with Reynolds number and 3D geometric effects. Also, both resonant and non-resonant conditions between vibrations in the two planes were taken into account. A similar treatment, though waiving (and questioning) the use of Reynolds number dependent terms, was presented by Carassale et al. (2005), who utilised Kronecker products and matrix calculus to derive a full aerodynamic damping matrix. Both these studies however focused on circular cylinders so the derivatives with respect to α were taken as zero so the results are not applicable to other galloping cases. It is worth referring also to Luongo and Piccardo (2005), who used bifurcation analysis to capture the limit cycle behaviour of detuned configurations, and to Caracoglia (2007), who extensively treated the galloping of

highway tubular poles while accounting for wind shear and coupling of along and across wind modes, again limited to Jones' (1992) schematic case with the principal axes along and perpendicular to the wind. These references, alongside broader 3DOF treatments, with different perspectives and not focusing on translational interaction (e.g. Wang and Lilien (1998), Yu et al. (1993)), cover the full range of available literature on modelling two-degree-of-freedom (2DOF) translational galloping vibrations. In summary, there has been no previous reference that has specifically (and correctly) addressed 2D translational galloping of non-circular cross sections with arbitrary orientation of the principal axes.

Other previous analysis of 2DOF coupled galloping has primarily been concerned with the combination of translational and rotational motions e.g. Blevins (1977), Blevins and Iwan (1974), Desai et al. (1990), McComber and Paradis (1998). However, in many cases there are similar structural conditions for translational motions in the two orthogonal planes normal to the cylinder axis and rotational motion may not occur simultaneously, so it is appropriate to consider pure translational 2DOF galloping. In this paper the correctly modified version of the Den Hartog criterion for an arbitrary angle of attack for 1D motion and a solution for the more generic motion in two orthogonal planes are derived in order to become a future reference for similar treatments. For simplicity and to emphasise the features of pure translational 2DOF galloping, potential rotational motion is not included. For the analysis the full aerodynamic damping matrix is formed and the scenario of coupled galloping oscillations is considered, which is shown to be a function of the structural parameters as well as the aerodynamic ones and can lead to elliptical trajectories.

2. Quasi-steady derivations

This paper aims to quantify the difference between the generalised 2DOF galloping scenario shown in Fig.2(a), not explicitly addressed before, and the normally considered special case in Fig.2(b) for pure across-wind motion. For completeness, the quasi-steady aerodynamic damping derivations, yielding galloping criteria, are briefly presented here, with an added intention of highlighting the errors in Eq.(2). Here the variation of the force coefficients with Reynolds number is neglected, since it is only relevant in special cases.

The classical Den Hartog derivation starts typically by writing the mean aerodynamic force, per unit length, along the y-axis in Fig.2, as a function of the mean drag and lift forces:

$$F_y = L\cos\alpha + D\sin\alpha \ , \tag{3}$$

where $L = \frac{1}{2}\rho U_{\rm rel}^2 B C_L$, $D = \frac{1}{2}\rho U_{\rm rel}^2 B C_D$, ρ is the fluid density, B is a reference dimension of the section

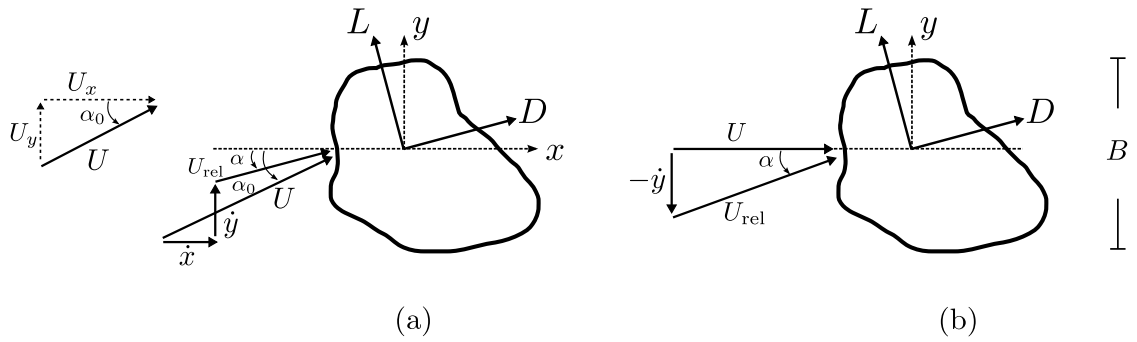

Figure 2: Geometry of a bluff section indicating lift and drag forces (L, D), relative angle of attack (α) and principal structural axes (x, y). (a) The general case with $\alpha_0 \neq 0$ and the potential for 2DOF motion. (b) The special case for 1DOF across-wind oscillations.

and $U_{\rm rel}$ is the relative velocity. Based on the quasi-steady assumption, F_y varies as a function of the body velocity, $\dot{y}$. Following Taylor series expansion of F_y around $\dot{y}$=0 and truncation of the higher order terms, which is deemed acceptable for small amplitude motion, the standard damped equation of motion of the body can be written as:

$$m\ddot{y} + c\dot{y} + m\omega_y^2 y = F_y = F_y|_{\dot{y}=0} + \dot{y} \cdot \left.\frac{dF_y}{d\dot{y}}\right|_{\dot{y}=0} , \tag{4}$$

where m is the cylinder mass per unit length, ω_y is the circular natural frequency (in the absence of wind), c is the structural damping coefficient, and overdots represent differentiation with respect to time. Not considering the nonlinear terms in Eq.(4) from the full Taylor expansion of the aerodynamic force F_y or from structural non-linearity, restricts its applicability to define the incipient instability, leaving the identification of any steady states aside. Exclusively when the free-stream wind velocity U and the motion velocity $\dot{y}$ are orthogonal and thus $\alpha = \arctan(-\dot{y}/U)$ (Fig.2(b)),

$$\left.\frac{dF_y}{d\dot{y}}\right|_{\dot{y}=0} = -\frac{1}{U}\, F_y'|_{\alpha=0} \ . \tag{5}$$

From Eq.(3), the derivative of F_y with respect to α, which can be used for Taylor expansion around any initial inclination α_0, is

$$F_y' = L' \cos\alpha - L \sin\alpha + D' \sin\alpha + D \cos\alpha \ . \tag{6}$$

In Eq.(4), the aeroelastic force (the last term on the right hand side), is equivalent to a linear viscous damping force. The condition for dynamic instability is simply that the total effective damping coefficient is negative. Hence from Eqs.(5&6), noting that for $\alpha = 0$, $U_{\rm rel}' = 0$, it is easily shown that the galloping

criterion is:

$$-\left.\frac{dF_y}{d\dot{y}}\right|_{\dot{y}=0} = \frac{\rho U B}{2}\left(C'_L + C_D\right) < -c\,. \tag{7}$$

For zero structural damping, this reduces to the classical Den Hartog criterion:

$$S_{\mathrm{DH}} = \left(C'_L + C_D\right) < 0\,. \tag{8}$$

which agrees with Eq.(2) for $\alpha = 0$.

If the motion is not normal to the wind direction, Eq.(7) does not hold and there are two problems with Eqs.(1&2). Firstly $\alpha \neq \arctan(-\dot{y}/U)$ so Eq.(5) is not valid, which affects both Eqs.(1&2). Secondly in finding L' and D', $U'_{\mathrm{rel}} \neq 0$, so extra terms are introduced in Eq.(2). For the general case of arbitrary orientation and for extending the analysis to cover two orthogonal translational DOFs (see Fig.2(a)), which potentially can lead to coupled response, the derivation follows. Note that x and y are the principal structural axes, which may or may not align with axes of symmetry of the cross-section. Rotation of the body has not been included.

In the general 2DOF translational case Eq.(3) still holds and also

$$F_x = -L\sin\alpha + D\cos\alpha. \tag{9}$$

after Taylor series expansion of F_y and F_x, again for small amplitude motion only retaining the linear viscous damping terms with the aim of identifying the stability of the initial at rest state, similar to before

$$\begin{aligned} F_y &= F_y|_{\dot{x}=\dot{y}=0} + \dot{x}\cdot\left.\frac{dF_y}{d\dot{x}}\right|_{\dot{x}=\dot{y}=0} + \dot{y}\cdot\left.\frac{dF_y}{d\dot{y}}\right|_{\dot{x}=\dot{y}=0}\,, \\ F_x &= F_x|_{\dot{x}=\dot{y}=0} + \dot{x}\cdot\left.\frac{dF_x}{d\dot{x}}\right|_{\dot{x}=\dot{y}=0} + \dot{y}\cdot\left.\frac{dF_x}{d\dot{y}}\right|_{\dot{x}=\dot{y}=0}\,. \end{aligned} \tag{10}$$

For evaluating the derivatives we employ the chain rule

$$\frac{d()}{d\dot{x}} = \frac{\partial()}{\partial U_{\mathrm{rel}}}\cdot\frac{dU_{\mathrm{rel}}}{d\dot{x}} + \frac{\partial()}{\partial\alpha}\cdot\frac{d\alpha}{d\dot{x}}\,, \tag{11}$$

and similarly for $\dot{y}$.

Keeping in mind the relations

$$U_{\rm rel} = \sqrt{(U_y - \dot{y})^2 + (U_x - \dot{x})^2}\ , \quad \tan\alpha = \frac{U_y - \dot{y}}{U_x - \dot{x}}\ , \quad \tan\alpha_0 = \frac{U_y}{U_x}\ , \tag{12}$$

finally the unit length full 2×2 aerodynamic damping matrix of a bluff section is obtained:

$$\mathbf{C}_{\rm aero} = \begin{bmatrix} c_{xx\rm a} & c_{xy\rm a} \\ c_{yx\rm a} & c_{yy\rm a} \end{bmatrix} = \begin{bmatrix} -\dfrac{dF_x}{d\dot{x}} & -\dfrac{dF_x}{d\dot{y}} \\ -\dfrac{dF_y}{d\dot{x}} & -\dfrac{dF_y}{d\dot{y}} \end{bmatrix}_{\dot{x}=\dot{y}=0} = \frac{\rho B U}{2} \begin{bmatrix} S_{xx} & S_{xy} \\ S_{yx} & S_{yy} \end{bmatrix}\ , \tag{13}$$

with

$$S_{xx} = C_D(1+\cos^2\alpha_0) - (C_L + C'_D)\sin\alpha_0\cos\alpha_0 + C'_L\sin^2\alpha_0\ , \tag{14a}$$

$$S_{xy} = -C_L(1+\sin^2\alpha_0) + (C_D - C'_L)\sin\alpha_0\cos\alpha_0 + C'_D\cos^2\alpha_0\ , \tag{14b}$$

$$S_{yx} = C_L(1+\cos^2\alpha_0) + (C_D - C'_L)\sin\alpha_0\cos\alpha_0 - C'_D\sin^2\alpha_0\ , \tag{14c}$$

$$S_{yy} = C_D(1+\sin^2\alpha_0) + (C_L + C'_D)\sin\alpha_0\cos\alpha_0 + C'_L\cos^2\alpha_0\ . \tag{14d}$$

To the authors' knowledge this full 2DOF translational aerodynamic damping matrix has not been succinctly and correctly presented previously. The derivation is also valid for wind skewed to the cylinder axis, by employing the wind component normal to the cylinder and the force coefficients with respect to that component, as long as the independence principle is a viable approximation.

The 1DOF instability thresholds for galloping in the pure x or y planes are simply when the diagonal terms of $\mathbf{C}_{\rm aero}$ become negative (or more generally equal to minus the structural damping coefficient). Evidently the non-dimensional aerodynamic damping coefficients, S_{xx} and S_{yy} in Eqs.(14a&d), differ from $S_{\rm sc}$ in Eq.(2), confirming that it is incorrect. For $\alpha_0 = 0$, S_{yy} in Eq.(14d) reduces to $S_{\rm DH}$ in Eq.(8) (as does S_{xx} in Eq.(14a) for $\alpha_0 = \pm 90°$), as expected.

For the instability condition of the coupled response, an eigenvalue analysis has to be performed for the 2DOF system, which is a function of the structural, as well as the aerodynamic, parameters. In general a numerical solution is required, but for special cases a closed form result is derived as follows. Since rotations are not included in this analysis potential inertial coupling of the degrees of freedom due to eccentricity of the centre of mass is not allowed for and the mass per unit length, m, associated with the two degrees of

freedom is the same. The equations of motion

$$m\ddot{x} + (c_x + c_{xa})\dot{x} + m\omega_x^2 x = -c_{xya}\dot{y} \ ,$$
$$m\ddot{y} + (c_y + c_{ya})\dot{y} + m\omega_y^2 y = -c_{yxa}\dot{x} \ , \tag{15}$$

with ω_x, ω_y and c_x, c_y the natural frequencies and structural damping coefficients for the two DOFs respectively, are assumed to possess a solution of the form

$$x = X\exp(\lambda t) \ , \quad y = Y\exp(\lambda t) \ , \tag{16}$$

where the eigenvalues λ and the amplitudes X, Y are in general complex-valued. Eqs.(15&16) then yield

$$\frac{Y}{X} = -\frac{\lambda^2 + \frac{c_{xx}}{m}\lambda + \omega_x^2}{\lambda\frac{c_{xya}}{m}} = -\frac{\lambda\frac{c_{yxa}}{m}}{\lambda^2 + \frac{c_{yy}}{m}\lambda + \omega_y^2} \ , \tag{17}$$

$$\lambda^4 + \left(\frac{c_{xx}+c_{yy}}{m}\right)\lambda^3 + \left(\frac{c_{xx}c_{yy} - c_{xya}c_{yxa}}{m^2} + \omega_x^2 + \omega_y^2\right)\lambda^2 + \left(\frac{c_{xx}\omega_y^2 + c_{yy}\omega_x^2}{m}\right)\lambda + \omega_x^2\omega_y^2 = 0 \ , \tag{18}$$

where $c_{xx} = c_x + c_{xa}$ and $c_{yy} = c_y + c_{ya}$. On the stability boundaries the eigenvalues are purely imaginary (λ=$i\omega$). When $\omega_x = \omega_y = \omega_n$, solving the biquadratic Eq.(18) for marginal stability gives

$$\omega = \omega_n \ , \quad \text{together with} \quad c_{xx}c_{yy} - c_{xya}c_{yxa} = 0 \ , \tag{19}$$

$$\text{or} \quad c_{xx} + c_{yy} = 0 \quad (\text{with } \omega \text{ not restricted to equal } \omega_n) \ . \tag{20}$$

For no structural damping ($c_x = c_y = 0$) Eq.(19) translates, in analogy to Eqs.(2, 8&14a&d), to the criterion for coupled galloping:

$$S_{2D} = \frac{1}{2}\left[3C_D + C_L' \pm \sqrt{\left(C_D - C_L'\right)^2 + 8C_L\left(C_D' - C_L\right)}\right] < 0 \ , \tag{21}$$

where S_{2D} denotes the non-dimensional effective aerodynamic damping coefficient of the coupled motion (equivalent to S_{xx} and S_{yy} for uncoupled motion) and the negative square root obviously gives the critical case. Here Y/X is real, indicating planar trajectories.

The solution in Eq.(20) corresponds to the so-called complex response (see Jones (1992), Macdonald and Larose (2008a)), which arises when the term under the square root in Eq.(21) is negative. Then the criterion

for coupled galloping (for no structural damping) becomes

$$S_{\mathrm{2D}} = \frac{1}{2}\left(3C_D + C'_L\right) < 0, \tag{22}$$

which coincides with the real part in Eq.(21), but in addition, the frequencies of the resulting two in-wind modes are released from being equal. This solution is often missed (as in Li et al. (1998), Liang et al. (1993)) by constraining X and Y to be real. From Eq.(17), for $\lambda = i\omega$ with $\omega \neq \omega_n$, Y/X is complex, indicating elliptical trajectories. Since the two modal responses occur simultaneously at different frequencies, a 2D beating-type behaviour occurs, as described in Jones (1992), Luongo and Piccardo (2005) and Macdonald and Larose (2008a).

More generally, in the presence of structural damping (the same in both planes, $c_x = c_y = c$), the right hand side of Eqs.(21&22) becomes $-2c/\rho BU$ (equivalent to Eq.(7)).

Also of interest is the case where the initial natural frequencies (or the structural damping) in the two DOFs (ω_x and ω_y or c_x and c_y) are not equal. Then on the stability boundary Eq.(18) yields:

$$(c_{xx}c_{yy} - c_{xy\mathrm{a}}c_{yx\mathrm{a}})(c_{xx} + c_{yy})(\kappa^2 c_{xx} + c_{yy}) + c_{xx}c_{yy}(1-\kappa^2)^2 m^2\omega_x^2 = 0, \tag{23}$$

where $\kappa = \omega_y/\omega_x$. This can generally only be solved numerically. For all detuned cases, the trajectories become elliptical, similar to actual occurrences of galloping in the field.

2.1. Relevance to uniform continuous systems

It is worth noting that all the derived aerodynamic damping estimates (and hence the galloping criteria), although referring explicitly to a unit length section, are often also applicable for a uniform continuous system allowing motion in two orthogonal planes, in a uniform flow. This can be easily proved by applying in Eqs.(15) the standard separation of time and space variables,

$$x(s,t) = \sum_n \phi_{x_n}(s) q_{x_n}(t)\ , \quad y(s,t) = \sum_n \phi_{y_n}(s) q_{y_n}(t), \tag{24}$$

where s is the distance along the continuous system, $\phi_{x_n}(s)$ and $\phi_{y_n}(s)$ are the n^{th} undamped mode shapes in the x, y planes and $q_{x_n}(t)$, $q_{y_n}(t)$ the corresponding generalised displacements. In addition to the standard orthogonality conditions for same-plane modes

$$\int m\phi_{x_{n_1}}(s)\phi_{x_{n_2}}(s)ds = 0 \ \text{ for } \ n_1 \neq n_2\ , \quad \int m\phi_{y_{n_1}}(s)\phi_{y_{n_2}}(s)ds = 0 \ \text{ for } \ n_1 \neq n_2\ , \tag{25}$$

for the case that the mode shapes in the two planes are the same (i.e. $\phi_{x_n}(s) = \phi_{y_n}(s) = \phi_n(s)$), which is common for uniform sections, for any pair of modes in the two planes, Eqs.(15) transform to

$$\ddot{q}_{x_n}(t)\int m(\phi_n(s))^2 ds + \dot{q}_{x_n}(t)\int c_{xx}(\phi_n(s))^2 ds + \omega_x^2 q_{x_n}(t)\int m(\phi_n(s))^2 ds = -\dot{q}_{y_n}(t)\int c_{xy\mathrm{a}}(\phi_n(s))^2 ds \ ,$$

$$\ddot{q}_{y_n}(t)\int m(\phi_n(s))^2 ds + \dot{q}_{y_n}(t)\int c_{yy}(\phi_n(s))^2 ds + \omega_y^2 q_{y_n}(t)\int m(\phi_n(s))^2 ds = -\dot{q}_{x_n}(t)\int c_{yx\mathrm{a}}(\phi_n(s))^2 ds \ . \quad (26)$$

Since for a uniform section in a uniform wind, the mass per unit length and damping coefficients (including aerodynamic components) are not functions of s, the integral term $\int (\phi_n(s))^2 ds$ cancels out, yielding back again Eqs.(15) and thus rendering the deduced instability thresholds in Eqs.(14a&d, 21&22) still valid. It is noted that when the aerodynamic damping coefficients cannot be deemed as constants over the structural length, as for instance for tall structures where the wind velocity profile is significant (varying the factor $\rho BU/2$), or for a varying section, then the integrals in Eq.(26) should be calculated explicitly. However, in many cases the simplifying approach of uniform wind velocity and section is adequate, and in the present situation it allows comparison between the relatively simple different criteria presented above.

3. Application: quantifying differences between the criteria

The differences in the results arising from the different galloping criteria are quantified by utilising data of aerodynamic force coefficients for a variety of cross-sectional shapes. Fortunately such data are available in the literature for many shapes (e.g. see Alonso et al. (2005, 2009), ESDU 82007 (2004), Jones (1992), Norberg (1993), Richardson and Martuccelli (1965), Tatsuno et al. (1990)), although they have almost exclusively been used in the Den Hartog criterion only, which, as previously stated, is not always the case in hand. For the current study a number of representative shapes, as illustrated in Fig.3, were chosen to span a whole range of possible relative differences between the different galloping criteria. The last three iced cable shapes (Figs.3(j,k,&l)), although only specific examples of the infinite number of possible iced geometries, were chosen for direct comparison with the similarly scoped work of Jones (1992), since, although she attempted to define the worst case for 1DOF or perfectly tuned coupled galloping, she chose a presentation method that did not make the actual differences in the results clear.

Fig.4 presents the non-dimensional aerodynamic damping coefficients for each galloping criterion, for

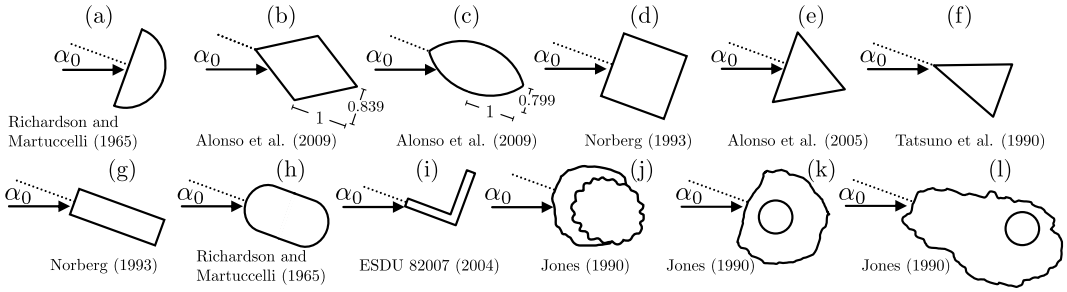

Figure 3: Sections with aerodynamic coefficients provided in the literature Alonso et al. (2005, 2009), ESDU 82007 (2004), Jones (1992), Norberg (1993), Richardson and Martuccelli (1965), Tatsuno et al. (1990), used in the galloping analysis herein.

each section, for the whole angle range of angles of attack that are available. Negative values identify aerodynamically unstable regions, where galloping would occur in the absence of structural damping. More generally, with structural damping, galloping occurs when the non-dimensional aerodynamic damping coefficient is below $-2c/\rho BU$. For each shape, three lines are plotted, corresponding to the aerodynamic damping contributions from: i) the classical Den Hartog summation, S_{DH}, in Eq.(8); ii) the more adverse of the two rotated 1DOF cases, S_{xx} or S_{yy}, as given in Eqs.(14a&d); and iii) the perfectly tuned 2DOF coupled motion case, S_{2D}, in Eqs.(21&22). It is pointed out that these correspond to three conceptually different motion scenarios: i) applies for different aerodynamic angles of attack of the cross-section, α, but with the motion always constrained to be purely across-wind; ii) applies to the instance where the principal structural axes and cross-sectional shape are fixed to each other and rotate together with respect to the wind (or the wind rotates relative to the structural axes and shape) as in Fig.2(a), with α_0 becoming the variable; and iii) applies to combined 2D motion with perfect tuning of the structural natural frequencies in the two planes, in which case the orientation of the structural axes is arbitrary, reflected by Eqs.(21&22) being independent of α_0, and only the orientation of the cross-sectional shape with respect to the wind direction then being relevant. The subcase of the 2DOF complex response (Eq.(22)) is distinguished in Fig.4 by plotting open circles on the line. It is notable that there is no case of instability linked to this scenario (i.e. S_{2D} from Eq.(22), when it applies, is never negative). This is keeping with the suggestion by Macdonald et al. (2008), for galloping of a skewed stranded cable in the critical Reynolds number range, that the combination of parameters required for galloping of a complex response is unlikely to occur in practice. In addition, comparing Eqs.(8&22), since C_D is always positive, the condition for 2DOF complex galloping is always less onerous than the condition for pure across-wind galloping. Hence, in contrast to Jones' (1992) suggestion that observations of elliptical galloping trajectories in the field can be attributed to complex galloping, here it seems probable that this is not the actual case.

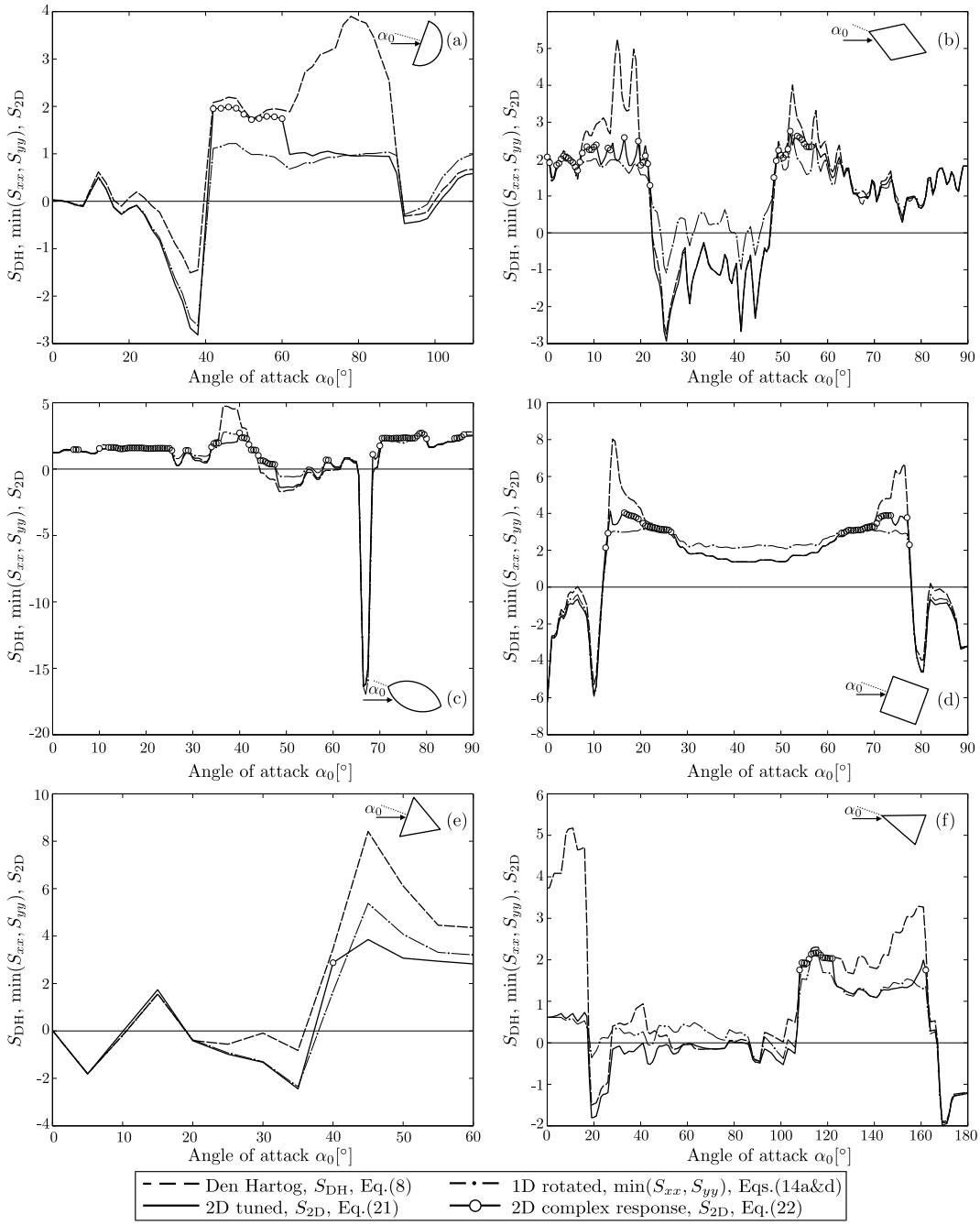

Figure 4: Non-dimensional aerodynamic damping coefficients (S_{DH}, min(S_{xx}, S_{yy}), S_{2D}) as a function of angle of attack for the cross-sectional shapes given in Fig.3 (inset letters link the two figures). Negative values indicate unstable behaviour (in the absence of structural damping).

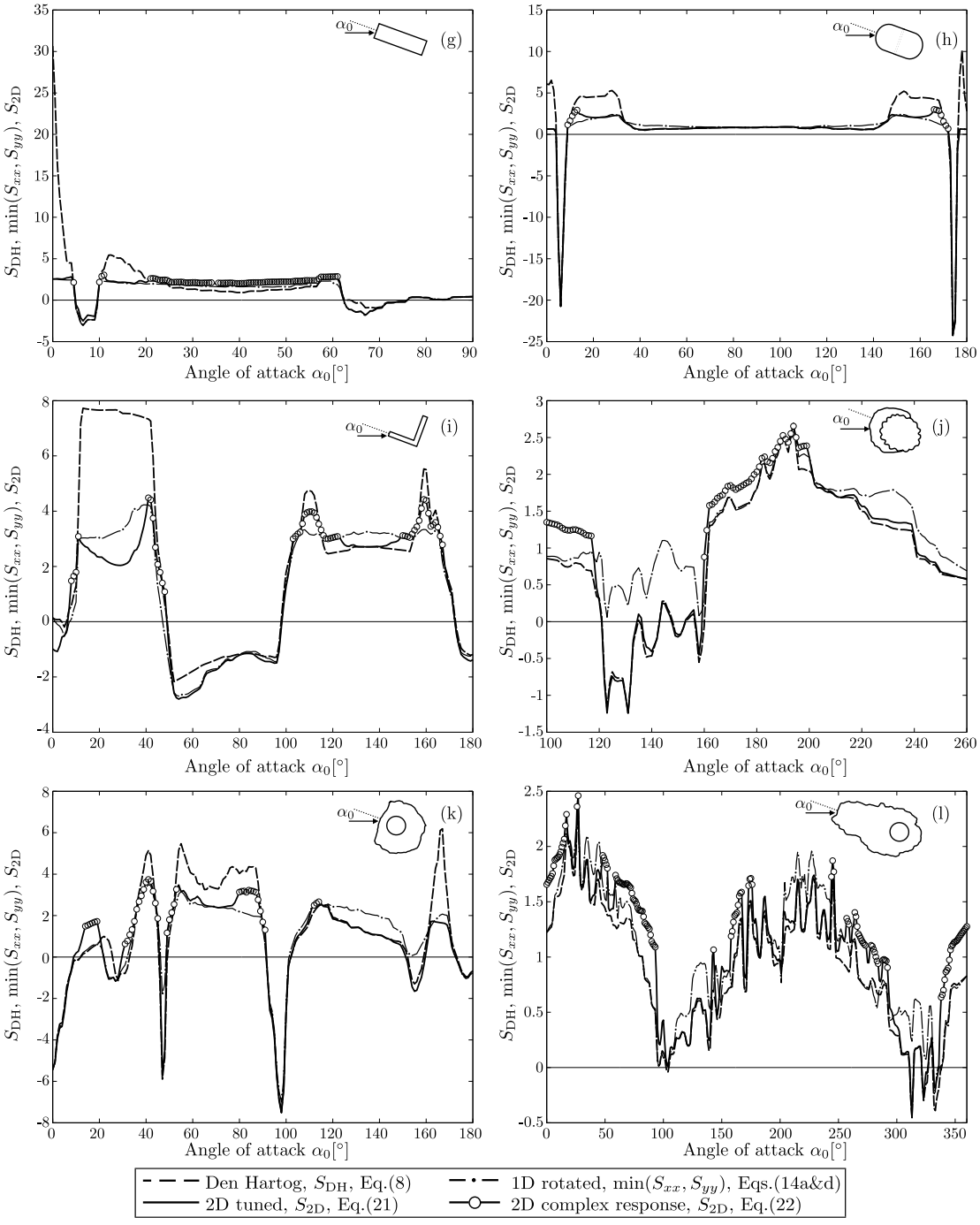

Figure 4 (continued)

The results presented here are for the cases of the wind and motion direction fixed at right angles to each other (case i), for the principal structural axes and cross-sectional shape fixed to each other (case ii) (relevant to slender bodies in bending, where the cross-sectional shape dictates both the aerodynamic and the structural stiffness), or for perfect tuning in 2DOF (case iii). However, the generalised approach allows the wind direction, principal structural axes and the orientation of the cross-sectional shape to all be independent. This could occur, for example, for a transmission line, where the wind is close to horizontal, the structural axes are given by the inclination of the cable catenary in the mean wind (Fig.1(b)), and the cross-sectional shape can rotate due to the influence of gravity on any accreted ice. Such a situation is still covered by Eqs.(13-15), where in Eq.(14) α_0 is the angle between the wind direction and the structural x-axis (Fig.2(a)), but C_D, C_L and their derivatives should be evaluated at the angle of attack between the wind direction and the reference direction of the cross-sectional shape (not necessarily equal to α_0 due to the cross-section rotating).

Commenting on the individual plots in Fig.4, the first impression is that in most cases all the values follow roughly similar trends and predict close instability zones with respect to the angle of attack. Especially for sections being or resembling rectangles, including the square in Fig.4(d), the rectangle with side ratio 3:1 in Fig.4(g), and the rectangle with rounded ends in Fig.4(h), the ranges of angles of attack for instability from the three different criteria are almost indistinguishable, showing some insensitivity of the susceptibility to galloping for the different cases. The square and rectangle were actually chosen for this study for exhibiting different characteristics, with the square galloping for zero angle of attack and the 3:1 rectangular not (for a classical treatise on the instabilities of rectangular sections with different side ratios see Nakamura and Hirata (1964)), although the most severe zone of instability is for an angle of attack near 10° in both cases. This is the case for the section in Fig.4(h) also. A similar connection exists between the rectangle in Fig.4(g) and the ellipsoid in Fig.4(c) with stronger instability near 70° for both, showing that sections with rounded faces can still exhibit negative aerodynamic damping values and consequently unstable behaviour, in this case likely because, after separation at the sharp corner, the flow then does not reattach, causing a rapid drop in lift. In any case, for all the figures referenced so far, the differences are sufficiently small to consider that any of the above instability bounds works quite well in any actual case. Indeed the previous lack of a study to quantify the differences arising from the use of different criteria can probably be linked to the fact that benchmark studies of galloping analysis have often been performed on rectangles or rectangle-like shapes, where the differences are unimportant.

On the other hand, another section, equally widely studied in wind tunnel tests and historically connected

with galloping, the D-section in Fig.4(a), shows more diverse behaviour. For zero angle of attack, the Den Hartog summation (S_{DH}) predicts zero aerodynamic damping (the D-section is a hard oscillator, see Weaver and Veljkovic (2005), that, for motion exceeding a certain amplitude, will gallop even for this angle of attack, but this is beyond the scope of the current analysis). Evidently the lesser of S_{xx} or S_{yy} (in this case S_{yy}) from Eqs.(14a&d) (referred to as the 1D rotated case hereafter) becomes the same as S_{DH} when $\alpha_0 = 0$, and slightly more unexpectedly the 2DOF solution (S_{2D}) also falls on the same value giving a common start for all three. As the angle of attack increases, S_{DH} departs from the other two, which have a negative peak near 40°, representing almost twice the negative aerodynamic damping as for S_{DH}. This is a significant difference and it clearly demonstrates that the appropriate galloping criterion should always be applied carefully to the actual problem in hand. Increasing the angle of attack further, a smaller instability zone is expected near 100° where now the most severe condition is for 2D motion and the Den Hartog summation estimates slightly more negative aerodynamic damping than for the 1D rotated case. Near 80° it is seen that S_{DH} gives extremely positive aerodynamic damping. Looking more broadly it is seen that for nearly all sections the Den Hartog summation gives the highest positive aerodynamic damping value. Such extreme values are often very close to the ones from the alternate 1D rotated case (the greater of S_{xx} or S_{yy}), which is not shown in Fig.4, which only presents the worse case. This also explains why in Figs.4(f,g&h) the Den Hartog summation does not match the 1D rotated case for zero angle of attack - the aerodynamic damping of along-wind vibrations is lower than for across-wind, although both are positive.

Other sections considered also show notable differences between the outputs for the different cases. The results for the triangle with a vertex angle 30° as shown in Fig.4(f) show that near 20° the 1D rotated case is close to being stable while the other two cases are clearly unstable, and around 30° the 2D case is unstable whereas the other two are not. The same section near 180° (presenting a flat face to wind) on the other hand shows all the three lines in Fig.4(f) coinciding. Similarly the equilateral triangle (Fig.4(e)) exhibits significant differences, although the 1D and 2D rotated cases generally give close results. In addition it is of interest to note that the two triangles behave quite differently (Fig.4(e&f)) when presenting their flat faces to the wind although only a small vertex angle change has occured. Differences are also apparent in Figs.4(b,j&k), with the 1D rotated case giving the least unstable results, thus rendering the simple Den Hartog calculation to be unnecessarily conservative if the structural axes rotate with the section. Conversely for the L-section in Fig.4(i), in the most critical region near 60°, the Den Hartog summation is unconservative.

Drawing some general conclusions, although in most cases the broad picture from the three criteria is similar, the absolute aerodynamic damping values at certain angles can be quite different. There are many

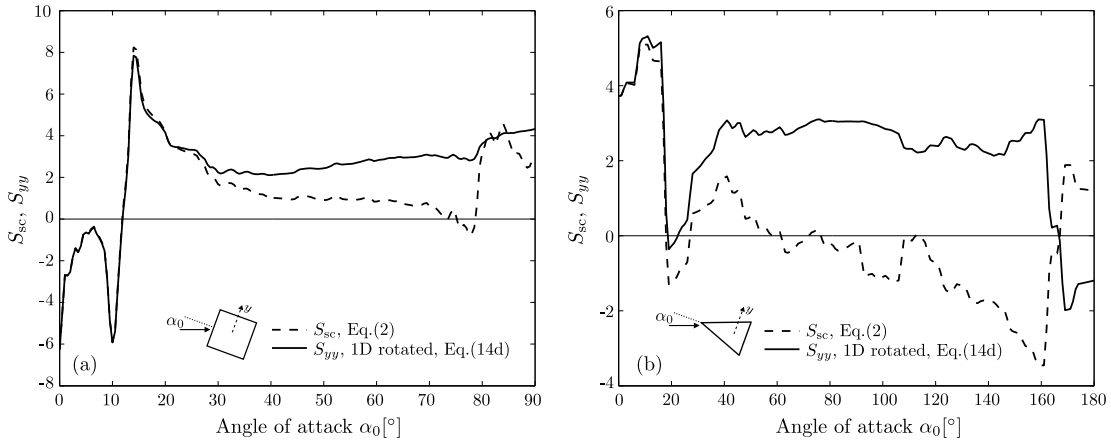

Figure 5: . Comparison between the erroneous S_{sc} (Eq.(2)) and the correct value for the 1D rotated y-axis case, S_{yy} (Eq.(14d)), for (a) the square in Fig.3(d) and (b) the triangle in Fig.3(f).

instances where a section stable according to one criterion can be unstable according to another, and there is no set sign for the relative differences, with changes being possible even for the same shape in a different range of angle of attack. Still, in almost all the examples interestingly the worst case occurs for the 2DOF criterion.

It should be noted that the accuracy of the results is of course limited by the accuracy of the available data. But additionally there is the need to convert the discrete point measurements of static force coefficients into a continuous or piecewise continuous function in order to determine their derivatives. Many options were considered for this purpose, including polynomial and harmonic curve fits of different orders. In any case there is a need for a high order for any function to accurately fit the measured points, which was recognised early by Blevins and Iwan (1974). In Blevins' analysis the nonlinear terms enter the equation of motion and subsequently solutions are sought to yield the steady state amplitudes, thus it is detrimental that the introduction of different non-linearity, from different fitted functions, strongly influences the results. However for the purposes of the present analysis, the different options make little difference to the results of the comparison (except making the plots smoother). For this reason the simplest possible, piecewise linear assumption was chosen for estimation of the derivatives in Fig.4.

Returning to the misleading galloping criterion in Eq.(2), it is useful to show the potential error arising from its use. At first sight it is clear that for 180° rotation it is the opposite of the Den Hartog criterion, while for 90° any correlation with the Den Hartog criterion should be deemed as fortuitous. Judging from the general similarity found between the Den Hartog case and the 1D rotated case, it is expected that great differences from Eq.(2) can emerge for $\alpha \neq 0$. Actually it should be noted that the correct direct equivalent

of Eq.(2) is not the worse of Eqs.(14a&d), as considered above, but only Eq.(14d), for motion in the y direction. As can be seen in Fig.5(a), showing the results from Eqs.(2&14d) for the square section, although Eq.(2) inaccurately predicts a weak instability zone near 80° it otherwise predicts instabilities in agreement with the correct result. This is only because a square's critical zone occurs for small angles of attack, where Eq.(2) should be close to the Den Hartog criterion. On the other hand, for the triangular section in Fig.2(f) the errors are alarming (Fig.5(b)). Apart from the initial agreement of the two curves for small α, Eq.(2) is consistently unable to capture not only the value of the aerodynamic damping but even its correct sign. This is true for most of the section shapes considered (Fig.3).

4. The effect of frequency detuning

The 2DOF solution presented above is restricted to perfectly tuned natural frequencies and equal structural damping coefficients in the two motion planes. It is evident that in a great number of situations different natural frequencies exist for the different directions of motion. Such a case is found for instance for cables, where, due to sag, the frequencies of odd in-plane modes are higher than for the corresponding out-of-plane ones. For any detuning the coupled Eqs.(15) still apply, but for increasing detuning the coupling terms on the right hand side become further from the relevant natural frequency and hence have a reduced effect on the behaviour. Eventually, for greatly detuned systems the coupling becomes irrelevant and the system behaves like two uncoupled 1DOF systems in the orthogonal planes. This poses the interesting questions of: i) what happens for close but not equal natural frequencies and ii) what will the behaviour be for quite large detuning values.

Utilising Eq.(23) for all the different sections in hand it is found that the two 1DOF and the tuned 2DOF solutions define an envelope within which the detuned coupled solutions always fall. The actual evolution with detuning consists of starting from the tuned 2DOF solutions (using $\pm$ in Eq.(21)) for zero detuning and progressively converging towards the 1DOF ones for large detuning, as presented, for example, in Fig.6(a) for the iced cable section of Fig.3(j) for an angle of attack of 123° (other parameters (m, ω_x, ρ, B, U) were taken from Jones (1992)). The alternate form of the solution is given for example in Fig.6(b) for the iced cable section of Fig.3(k) for an angle of attack of 30°, where one of the 1D solutions is more onerous than the 2D tuned ones (similar beneficial or detrimental effect of detuning on galloping thresholds was previously also observed for the case of tubular poles in Caracoglia (2007)). The actual rate of convergence is found to be strongly dependent on the force coefficients and hence the angle of attack. The smaller the initial difference between the coupled and uncoupled solutions in Fig.4, the slower the rate of convergence seems

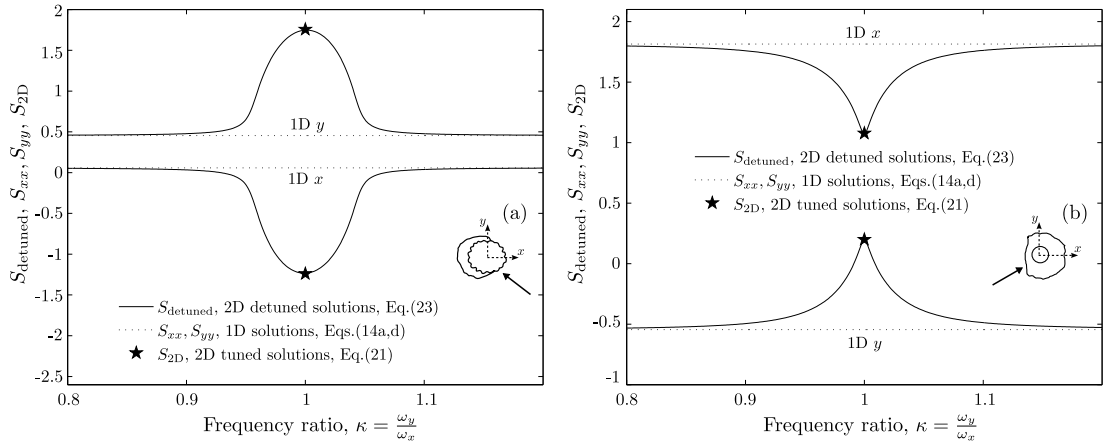

Figure 6: Evolution of the non-dimensional aerodynamic damping coefficient for different values of detuning, κ, for (a) the section in Fig.3(j) at $\alpha = 123°$ and (b) the section in Fig.3(k) at $\alpha = 30°$. The lower branch is the critical one. In (a) for perfect tuning the solution is unstable (negative aerodynamic damping) and for detuning above about 7% it approaches the 1D solution, which in this case is stable. In (b), on the other hand, for perfect tuning the solution is stable and for detuning above 1% it becomes unstable while approaching the 1D solution.

to become. As clearly shown in Fig.6(a), for detuning of only 7% the 2D solution, which is unstable when tuned, becomes stable and approaches the 1D solution (see the lower critical branch in the figure and also Fig.4(j) at 123°).

Incidentally, this particular example gives the opportunity to correct an erroneous conclusion reached by Jones (1992). Results from tests on this section by Nigol and Buchan (1981), where no galloping occurred, were taken as support for an assertion that in general when along-wind motion is restrained then no instability can ever occur. However, the reasoning was only a result of forgetting the associated external restraining force in the balance of forces in the equation of motion. As seen in Fig.4(j) at 123°, picked as being the most critical orientation, the tuned 2D solutions and Den Hartog criteria produce indistinguishable values. Thus in this case, with allowance for across-wind motion, presence or absence of along-wind motion, whatever the frequency ratio between the two, hardly changes the galloping threshold. The true reason for the lack of observed galloping in this case, which is theoretically only slightly unstable, is likely related to the level of structural damping and/or slight inaccuracies in quasi-steady theory when hybrid vortex-buffeting-galloping mechanisms are involved, as discussed by Bearman et al. (1987) and Luo et al. (1998).

Finally in this section it is interesting to discuss the response trajectories, which as already mentioned can range from planar to elliptical. As discussed above and shown in Fig.6, for quite small detuning the 2D solutions quickly approach the aerodynamic damping values that correspond to the 1D solutions. However, they still remain qualitatively different from them in terms of the trajectories, which are described by

Eq.(17). The evolution of the trajectories are presented for the case of Fig.6(a) in Fig.7. When perfectly tuned (Fig.7(a)), two planar modes occur (not necessarily in orthogonal planes). For small detuning values, the planar motion of the modes turns into ellipses with growing magnitudes of their minor axes as the detuning increases. This is shown for $\kappa = 1.005$ in Fig.7(b). For larger detuning the axes of the elliptical modes also rotate as in Fig.7(c), where $\kappa = 1.05$. This rotation continues until the principal structural axes are reached, and when that is virtually accomplished (for a frequency ratio of the order of 1.1 in this case as in Fig.7(d)) the width of the ellipses reduces as they converge onto the uncoupled planar solutions. The aerodynamic damping coefficients have virtually converged on the 1D solutions for frequency rations of about 1.1 (and 0.9), but the detuning values required to produce essentially planar responses are in fact much larger (frequency ratios of the order of 3 or 1/3 in this case). The relevant aerodynamic damping coefficients are shown in Fig.7 to indicate instabilities and to establish the link to Fig.6(a). It is a noteworthy conclusion that the elliptical galloping paths observed in the field (see discussion in Jones (1992)), are almost certainly due to the effect of detuning between the structural axes.

5. Conclusions

Quasi-steady aerodynamic theory, which lies at the core of the current analysis, has known limitations and it has long been recognised that in certain operational ranges (only approximately identifiable) it breaks down. Still, for a broad range of conditions for low frequency modes, quasi-steady analysis has a proven ability to predict aerodynamic damping and galloping behaviour. The role of the current paper is to identify cases where limitations are introduced only because of shortcomings in the actual application of the method and to consider its generalisation for 2DOF translational motion with arbitrary orientation of the principal structural axes.

The case sketched in Fig.2(a), with the structural axes inclined to the wind direction, has hardly been considered before and the differences in the behaviour from classical across-wind galloping had not been quantified. Application of the Den Hartog galloping criterion, or even worse an erroneous extension of it presented in Eq.(2), for the rotated system or wind, can yield solutions that can range from close to even the opposite of the correct generalised ones. Although the Den Hartog summation often gives reasonable estimates of the aerodynamic damping even for the rotated case, it can in some circumstances give negative estimates of only around half the magnitude of the real values, which is potentially unsafe. Conversely in some other cases it can be unnecessarily conservative. Furthermore, the dynamic stability of a section can be determined not only by its shape, the aerodynamic orientation and the orientation of the principal

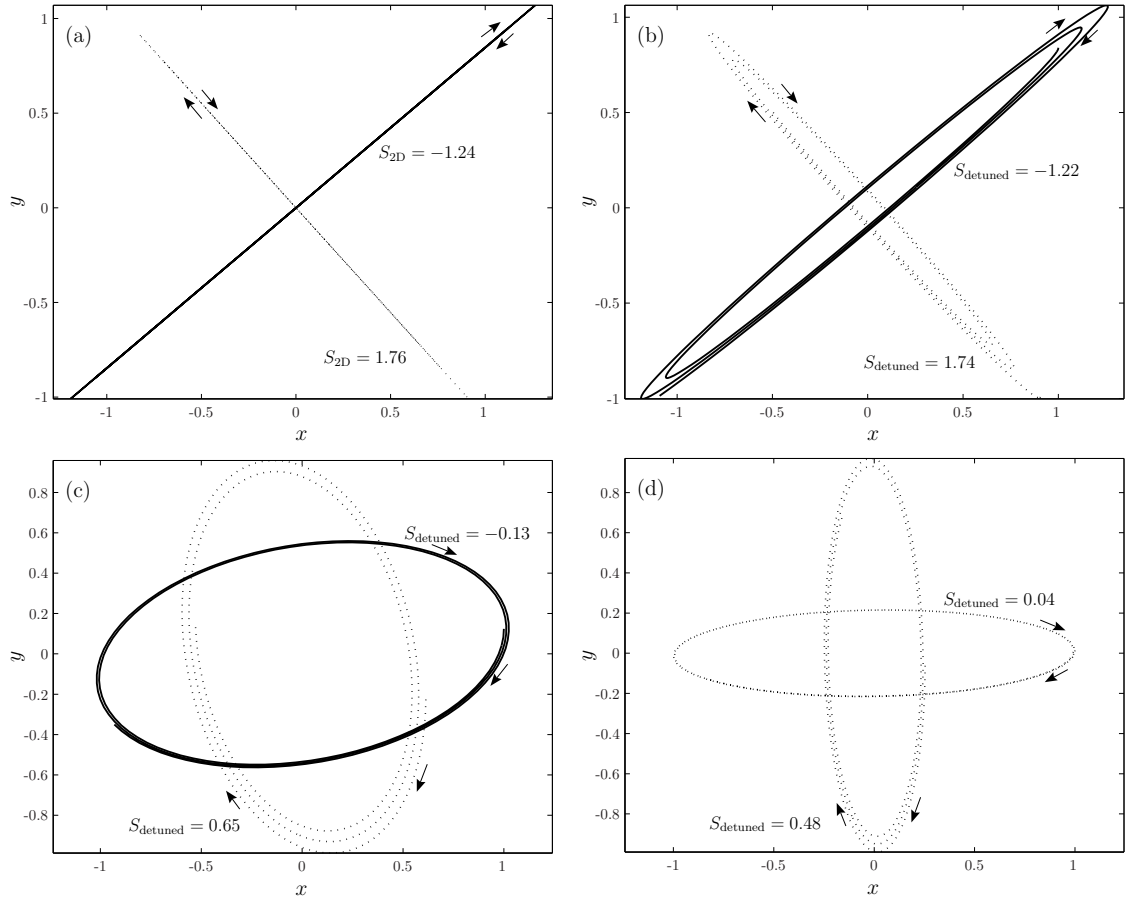

Figure 7: Modal trajectories corresponding to Fig.6(a) for $c_x = c_y = 0$ and (a) $\kappa = 1$, (b) $\kappa = 1.005$, (c) $\kappa = 1.05$ and (d) $\kappa = 1.1$. The corresponding S_{detuned} value is also indicated for each mode. Unstable modes are plotted with solid lines while stable ones are dotted. Note for comparison that $S_{xx} = 0.45$, $S_{yy} = 0.06$.

structural axes (which may or may not follow the aerodynamic orientation), but also by the proximity of the structural natural frequencies in the two planes.

The correct equations for the non-dimensional aerodynamic damping coefficients, and hence the dynamic instability criteria, have been derived for an arbitrary orientation of the system with respect to the wind, and they have been evaluated for a range of sections for perfectly tuned and well detuned natural frequencies. Such a presentation (not previously existing as such) is valuable for understanding the way galloping behaviour is dependent on the geometric arrangement details and frequency tuning. Furthermore, detuning has received very little attention in the existing literature. Here, detuned results, numerically obtained, have been shown always to fall between the solutions for the 2D perfectly tuned case and the two uncoupled 1D cases, so the most critical of the 1D or perfectly tuned 2D cases can be used conservatively. The equations provided are almost as easy to apply as the classical Den Hartog equation, yet they avoid potential errors and give accurate estimates of the aerodynamic damping and the propensity of a cylinder to gallop. But it is important to use the particular equation relevant to the specific problem being addressed.

References

Alonso, G., Meseguer, J., and Pérez-Grande, I. (2005). Galloping instabilities of two-dimensional triangular cross-section bodies. *Exp. Fluids*, 38:789–795.

Alonso, G., Valero, E., and Meseguer, J. (2009). An analysis on the dependence on cross section geometry of galloping stability of two-dimensional bodies having either biconvex or rhomboidal cross sections. *Eur. J. Mech. B/Fluids*, 28:328–334.

Bearman, P., Gartshore, I., Maull, D., and Parkinson, G. (1987). Experiments on flow-induced vibration of a square-section cylinder. *J. Fluid Struct.*, 1:19–34.

Blevins, R. (1977). *Flow-Induced Vibrations*. Van Nostrand, New York, 1st edition.

Blevins, R. and Iwan, W. (1974). The galloping response of a two-degree-of-freedom system. *J. App. Mech.*, 41:1113–1118.

Caracoglia, L. (2007). Influence of weather conditions and eccentric aerodynamic loading on the large amplitude aeroelastic vibration of highway tubular poles. *Eng. Struct.*, 29:3550–3566.

Carassale, L., Freda, A., and Piccardo, G. (2005). Aeroelastic forces on yawed circular cylinders: Quasi-steady modeling and aerodynamic instability. *Wind Struct.*, 8(5):373–388.

Davenport, A. (1966). The treatment of wind loading on tall buildings. In *Symposium on Tall Buildings*, pages 3–45, University of Southampton, England. Pergamon Press.

Den Hartog, J. P. (1932). Transmission line vibration due to sleet. *Trans. AIEE*, 51:1074–1086.

Den Hartog, J. P. (1947). *Mechanical Vibrations*. McGraw-Hill, New York, 3rd edition.

Desai, Y., Shah, A., and Popplewell, N. (1990). Galloping analysis for two-degree-of-freedom oscillatior. *J. Eng. Mech.-ASCE*, 116:2583–2602.

ESDU 82007 (2004). *Structural members: mean fluid forces on members of various cross sections*. Engineering Sciences Data Unit, London, UK.

Hémon, P. and Santi, F. (2002). On the aeroelastic behaviour of rectangular cylinders in cross-flow. *J. Fluid Struct.*, 16:855–889.

Holmes, J. (2001). *Wind Loading on Structures*. Spon Press, New York, 1st edition.

Jones, K. (1992). Coupled vertical and horizontal galloping. *J. Eng. Mech.-ASCE*, 118:92–107.

Li, Q., Fang, J., and Jeary, A. (1998). Evaluation of 2d coupled galloping oscillations of slender structures. *Comput. Struct.*, 66:513–523.

Liang, S., Li, Q., Li, G., and Qu, W. (1993). An evaluation of the onset wind velocity for 2d coupled oscillations of tower buildings. *J. Wind Eng. Ind. Aerodyn.*, 50:329–340.

Luo, S., Chew, Y., Lee, T., and Yazdani, M. (1998). Stability to translational galloping vibration of cylinders at different mean angles of attack. *J. Sound Vib.*, 215:1183–1194.

Luongo, A. and Piccardo, G. (2005). Linear instability for coupled translational galloping. *J. Sound Vib.*, 288:1027–1047.

Macdonald, J., Griffiths, P., and Curry, B. (2008). Galloping analysis of stranded electricity conductors in skew winds. *Wind Struct.*, 11(4):303–321.

Macdonald, J. and Larose, G. (2008a). Two-degree-of-freedom inclined cable galloping – Part 1: General formulation and solution for perfectly tuned system. *J. Wind Eng. Ind. Aerodyn.*, 96:291–307.

Macdonald, J. and Larose, G. (2008b). Two-degree-of-freedom inclined cable galloping – Part 2: Analysis and prevention for arbitrary frequency ratio. *J. Wind Eng. Ind. Aerodyn.*, 96:308–326.

McComber, P. and Paradis, A. (1998). A cable galloping model for thin ice accretions. *Atmos. Res.*, 46:13–25.

Nakamura, Y. and Hirata, K. (1964). The aerodynamic mechanism of galloping. *T. Jpn Soc. Aeronaut. S.*, 36(114):257–269.

Nigol, O. and Buchan, P. (1981). Conductor galloping part I - Den Hartog mechanism. *IEEE T. Power Ap. Syst.*, 100(2):699–707.

Norberg, C. (1993). Flow around rectangular cylinders: Pressure forces and wake frequencies. *J. Wind Eng. Ind. Aerodyn.*, 49:187–196.

Richardson, A. and Martuccelli, J. (1965). *Research study on galloping of electric power transmission lines*, volume II, pages 611–686. HMSO, London, UK.

Tatsuno, M., Takayama, T., Amamoto, A., and Koji, I. (1990). On the stable posture of a triangular or a square cylinder about its central axis in a uniform flow. *Fluid Dyn. Res.*, 6:201–207.

Wang, J. and Lilien, J. (1998). Overhead electrical transmission line galloping: A full multi-span 3-DOF model, some applications and design recommendations. *IEEE T. Power Deliver.*, 13(3):909–916.

Weaver, D. and Veljkovic, I. (2005). Vortex shedding and galloping of open semi-circular and parabolic cylinders in cross-flow. *J. Fluid Struct.*, 21:65–74.

Yu, P., Desai, Y., Shah, A., and Popplewell, N. (1993). Three-degree-of-freedom model for galloping. Part I: Formulation. *J. Eng. Mech.-ASCE*, 119:2404–2425.